 DOI: 10.1002/masy.200850504

Spectroscopical Investigation of Ski Base Materials

Jörg Fischer,[*1] *Gernot M. Wallner,*[2] *Alois Pieber*[3]

Summary: Raman spectroscopy was applied to perform a comprehensive morphological analysis of polyethylene (PE) ski base materials at different processing levels. The morphological characterization included determination and evaluation of Raman spectra and examination of the crystallinity values by differential scanning calorimetry (DSC). A good agreement between Raman and DSC crystallinity fractions was obtained, thus corroborating the Raman spectroscopy approach. While for the PE grade with the lowest average molar mass no significant morphological changes due to processing from the raw material via the extruded film to the post-treated film was found, higher molar mass PE grades exhibited a decrease of crystallinity, but an increase of the amorphous fraction along the process chain.

Keywords: DSC; morphology; polyethylene; Raman spectroscopy; ski base

Introduction

From a market point of view polyethylene (PE) is the most important commercially used polymer with overall market shares of about 30%.[1] While commodity PE grades are dominating in various industrial sectors, such as the packaging industry, engineering PE grades have also been developed for technical applications, requiring special functional properties. An outstanding example is ultra-high-molecular-weight polyethylene (UHMWPE) with advanced tribological behaviour. In the literature many investigations on UHMWPE are described focusing on the application as bearing material in orthopaedics.[2–6] However, PE grades with special tribological properties are also used for other applications which attract less scientific attention. Regarding the leisure and sports industry PE materials are of special relevance for running surfaces (i.e., bases), which are a key element of alpine and nordic skis determining their glide characteristics. For this application currently polyethylene extrusion grades with molar mass between 300,000 and 600,000 g/mol (high density polyethylene (HDPE)) and sinter grades with molar mass between 3,000,000 and 12,000,000 g/mol (UHMWPE) are used. The process from the raw material to a finished ski base surface consists of various steps, including the formulation and compounding of the material, the extrusion or sintering of semi-finished films, post-treatment (e.g., flaming) of the film, and production of the ski. To improve the base performance advanced material formulations and surface structuring techniques have been developed, implemented and used. While relationships between the additive content of ski base materials, the topographical structure of ski base surfaces and the gliding characteristics were established, up to now no systematic investigation on the effect of material morphology on the performance of ski base surfaces has been carried out. Hence, the overall objective of our research work is to study the morphology of ski base materials on different processing levels (raw material (compound), semi-finished film and post-treated film) by various techniques.

[1] Polymer Competence Center Leoben GmbH, Parkstrasse 11, Leoben, 8700, Austria
Fax: (+43) 3842 402 2102;
E-mail: jfischer@pccl.at
[2] Institute of Material Science and Testing of Plastics, University of Leoben, Franz-Josef-Strasse 18, Leoben, 8700, Austria
[3] Fischer GmbH, Fischerstrasse 8, Ried/Innkreis, 4910, Austria

HDPE and UHMWPE are linear forms of polyethylene with semi-crystalline morphology. Important variable parameters of semi-crystalline polymers are the degree of crystallinity and the semi-crystalline morphology, which is considered as a superposition of three phases, the crystalline component (often lamellae), the melt-like amorphous component and the disordered component of anisotropic nature (interphase).[7]

Relevant parameters of polyethylene are commonly derived by density measurement, differential scanning calorimetry (DSC), infrared (IR) and Raman spectroscopy, nuclear magnetic resonance spectroscopy (NMR), and wide and small angle X-ray scattering (WAXS and SAXS) techniques. While for most of these methods an adequate sample preparation (i.e., the destruction of the sample) is required, Raman spectroscopy has proved to be an appropriate tool to investigate morphological parameters of PE without any kind of damage. Furthermore, Raman spectroscopy allows for a rather comprehensive description of morphological parameters including the full characterization of the three phase components. Although there are some controversies in the literature concerning the feasibility of Raman spectroscopy for the determination of the disordered phase[8–10], various recent studies[6,11] have used the three phase model to describe morphology changes due to processing or loading and obtained reasonable results from a polymer physical point of view.

The sliding characteristic of ski bases is mainly affected by structural and morphological parameters of the surface layer, which is in contact with the snow counterpart. Therefore, the primary purpose of this paper is to describe morphological parameters at the surface of PE ski base grades as a function of different processing levels. In addition to the various advantages described above, Raman spectroscopy is a sensitive method with high lateral and vertical resolution to determine the morphology of materials surfaces. Therefore, Raman spectroscopy was applied in this study as the prime method. To corroborate the crystallinity values determined by Raman spectroscopy DSC measurements were also carried out. Regarding DSC special attention was given to the sample preparation. An appropriate technique to cut the sample from the surface layer was implemented and used.

Experimental Part

Materials

Within this work five polyethylene grades differing in their average molar mass and distribution were selected, compounded with additives but without modifiers (e.g., carbon black) and processed to semi-finished products (ski base film) (Table 1). The compounds and semi-finished products were supplied by Fischer GmbH (Ried, Austria). Depending on the material grade two different techniques, extrusion (200–220 °C) and sintering (200–230 °C, 250 bar, 12 h, heating/cooling rate: 30 °C/h) were applied to manufacture the ski base film, which was further treated (post-treated film) by flaming with an oxygen rich (yellow) flame (200–300 °C, 0.5–1 s). These processing steps are common before the production of the ski.

Table 1.
Characteristics of the polyethylenes used in this work.

Designation in this work	Material	Processing method	Density (g/cm^3)	$M_W \times 10^{-3}$ (g/mol)
M2	HDPE	extrusion	0.914	250
M4	HDPE	extrusion	0.936	400
H4	UHMWPE	sintering	0.911	4,000
H9	UHMWPE	sintering	0.918	9,000
HA	UHMWPE	sintering	0.918	10,500

Due to secrecy reasons further processes after the ski production are not considered within this paper.

Raman Spectroscopy

Raman spectra were determined by using a LabRam confocal-Raman spectrometer (HORIBA Jobin Yvon GmbH, Bensheim, D). Excitation of Raman bands was obtained upon irradiating the sample with a frequency doubled Nd-YAG laser of 100 mW operating at 532 nm. All measurements were performed in a backscattering geometry, using a 100× long working distance (3.4 mm) microscope objective with a numerical aperture value of 0.80, providing a lateral resolution of about 800 nm. To obtain a spectral resolution of about 3 cm^{-1} a diffraction grating of 1800 grooves/mm was used. Single point spectra were derived from 5 scans with an accumulation time of 5 s. By measuring on three different positions of a specimen mean and standard deviation values were evaluated.

The Raman spectra were manipulated by smoothing and baseline correction. To determine the areas under the peaks of interest, which was used as the measure for the intensity values (I), a curve-fitting procedure was carried out with the software package PeakFit v4.12 (SeaSolve Software Inc.). Appropriate fitting results were obtained by peak fitting with freely floating ratios of Gaussian and Lorentzian amounts automatically optimized by the software (Figure 1). The reproducibility of the fit was corroborated by fitting the peaks multiple times.

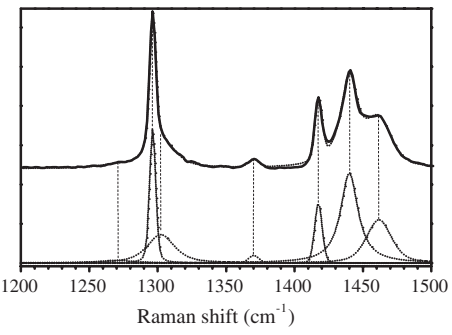

Figure 1.
Raman spectra of PE with typical curve fitting results.

To evaluate the degree of crystallinity (α_c) the method devised by Strobl and Hagedorn[7] was used (see Eq. (1)). Because ski bases are produced by at least partial melting and crystallization orthorhombic crystalline structures were assumed.

$$\alpha_c = \frac{I_c}{0.45 \cdot I_T} \cdot 100\% \quad (1)$$

where I_c is the integrated area of the Raman band representing the orthorhombic crystalline phase, I_T is the integrated area of the CH_2 twisting vibration region (1200–1350 cm^{-1}), which is not affected by the morphology and therefore used as an internal intensity reference and 0.45 is a normalization coefficient, which was found through experiments on 100% crystalline PE. [12,13]

Furthermore the fraction of the amorphous phase (α_a) was calculated by using Eq. (2)[7]:

$$\alpha_a = \frac{I_a}{I_T} \cdot 100\% \quad (2)$$

where I_a is the integrated area of the Raman band representing the amorphous phase.

Finally, the fraction of the interphase (α_b) is given by Eq. (3)[7]:

$$\alpha_b = 100\% - \alpha_a - \alpha_c \quad (3)$$

Differential Scanning Calorimetry

The DSC measurements were conducted on a Mettler Toledo DSC 822^e instrument (Mettler Toledo GmbH, Schwerzenbach, CH). Before testing, temperature and heat flow signals from the apparatus were calibrated using indium and zinc. Thermal analyses were carried out in air with PE specimens whose weight ranged between 2 and 3 mg. Samples with a thickness of 0.2 mm and a diameter of 4 mm were prepared from the semi-finished and post-treated films by planning a layer with the defined thickness and by cutting with the defined cross-section (diameter). Each DSC curve was recorded from −30 to 180 °C applying a heating rate of 10 °C/min. The degree of crystallinity

was determined as the ratio between the heat of fusion of the specimen and the heat of fusion of a perfect (100%) crystalline PE (293.6 J/g).[14] To check possible superimposed melting and crystallization effects due to a low heating rate, various heating rates ranging from 10 to 50 °C/min were applied in preliminary investigations. Because no effect of heating rate on the DSC based crystallinity values was found, the standardized rate of 10 °C/min was used. By measuring on three different specimens mean and standard deviation values were evaluated.

Results and Discussion

Raman Spectroscopy

As discussed in various references[2,4–7,11–13,15–20], in Figure 2 a representative Raman spectrum of PE material H9 is exhibited along with the assignment of the Raman bands to vibration modes. Attributions of Raman bands to morphological phases and to conformational states of the PE chains are well established.[2,4–7,11–13,15–20] In the spectral region from 1000 to 1550 cm^{-1} the bands between 1400 and 1480 cm^{-1} correspond to methylene bending vibrations ($\delta(CH_2)$). The crystalline phase is represented by the peak at 1416 cm^{-1} (crystallinity band)[7]. This band is in conjunction with a crystal field splitting phenomenon, which is resulting from an interaction between the two chains of the orthorhombic unit cell in all-trans conformation.[16] The crystallinity band at 1416 cm^{-1} has been used to determine the degree of orthorhombic crystallinity of PE samples.[2–13,15,19] For the monoclinic crystalline structure, which is a further lattice structure observed in PE, high chain folding energy is required. Hence, a direct crystallization from the melt into the monoclinic form is impossible. [5,21] A prerequisite for recrystallization from the orthorhombic to the monoclinic structure is a high energy input (i.e., shear or compression deformation).[22–24] For melt crystallized PE samples without significant energy input the orthorhombic crystallinity represents the overall crystalline fraction.

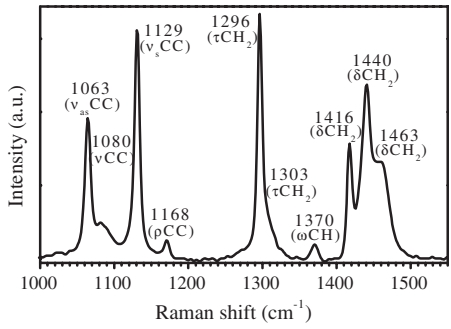

Figure 2.
Raman spectrum of PE together with indication of peak wavenumbers and vibration modes.

The bands at 1080 and 1303 cm^{-1} are assigned to the amorphous phase with PE chains in gauche conformation. Both bands have been used to determine the amount of the amorphous fraction. However, the values of the amorphous content derived from the band at 1303 cm^{-1} (amorphous band) are reported to be more reliable.[15] The Raman peaks at 1063 and 1123 cm^{-1} are attributed to the symmetric and asymmetric C–C stretching vibrations, respectively, occurring in conformational trans sequences longer than 10 all-trans bonds.[16,25] Because of the highly localized character of the methylene twisting vibrations ($\tau(CH_2)$), the peaks at about 1300 cm^{-1} are almost independent of conformation and temperature. Therefore, the integrated intensity of the methylene twisting bands is used as an internal intensity standard.

In Figure 3 Raman spectra of the investigated PE samples at the various processing levels are displayed. A qualitative interpretation of the crystalline and amorphous fractions is done by analysis of the spectral regions from 1400 to 1550 cm^{-1} (bending vibrations) and 1250 to 1350 cm^{-1} (twisting vibrations), respectively. For the semi-finished and post-treated films higher intensities of the amorphous band at 1303 cm^{-1} are observable.

Hence, due to extrusion or sintering of the raw material an increase of the amorphous phase is established. Concerning the crystallinity band no distinct trends

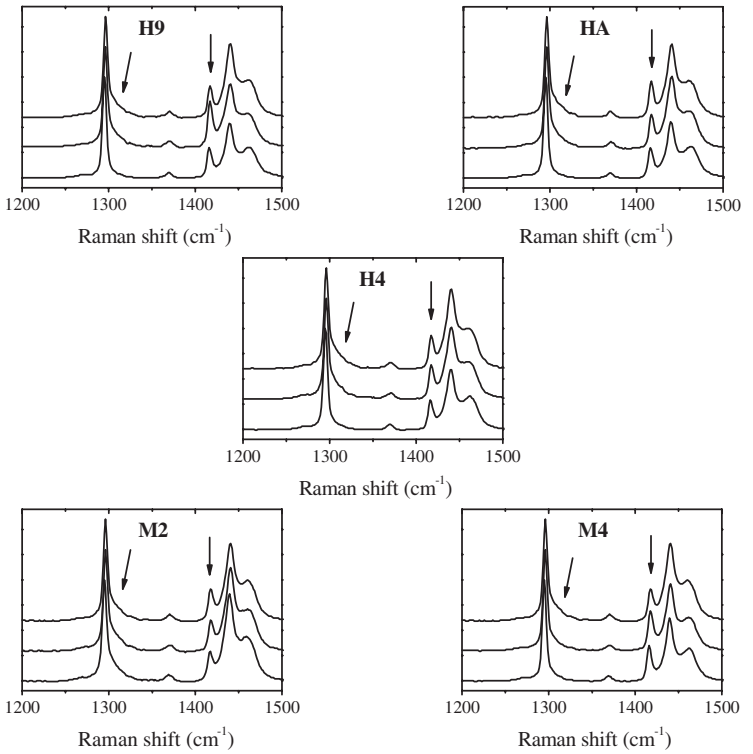

Figure 3.
Raman spectra of the investigated PE grades (M2, M4, H4, H9 and HA) at raw material, semi-finished film and post-treated film level (from bottom to top). The spectra are normalized to the internal intensity standard band at 1296 cm^{-1}.

along the process chain are ascertainable. Therefore, a comprehensive analysis of the three phases was carried out. Quantitative data of the crystalline, amorphous and interfacial contents for the investigated PE materials are revealed in Figure 4 and summarized in Table 2. For many of the investigated PE grades the highest crystallinity values but lowest amorphous fractions were obtained for the raw material (exception: M2 grade with the lowest average molar mass value). As an effect of film extrusion, sintering and post-treatment the crystallinity of the samples M4, H4, H9 and HA decreased whereas the content of the amorphous phase increased. Hence, the progresses of the crystallinity and amorphous content for polymers with an average molar mass higher than about 400,000 g/mol are following the same trend. Again, M2 with the lowest average molar mass exhibited a different trend with less significant changes in the crystalline and amorphous fractions. Regarding the interphase the highest values were established for the raw materials. Due to processing a tendency for a decrease of the interfacial content is observable.

As to the effect of average molar mass on the morphology, for the various raw materials the highest crystallinity value was obtained for the extrusion grade M4. For the UHMWPE grades slightly lower crystallinities, but higher interfacial fractions and thus the lowest amorphous contents were identified. The lowest crystalline fraction determined for the extrusion grade M2 with an average molar mass of only 250,000 g/mol is presumably related to a higher branching density.

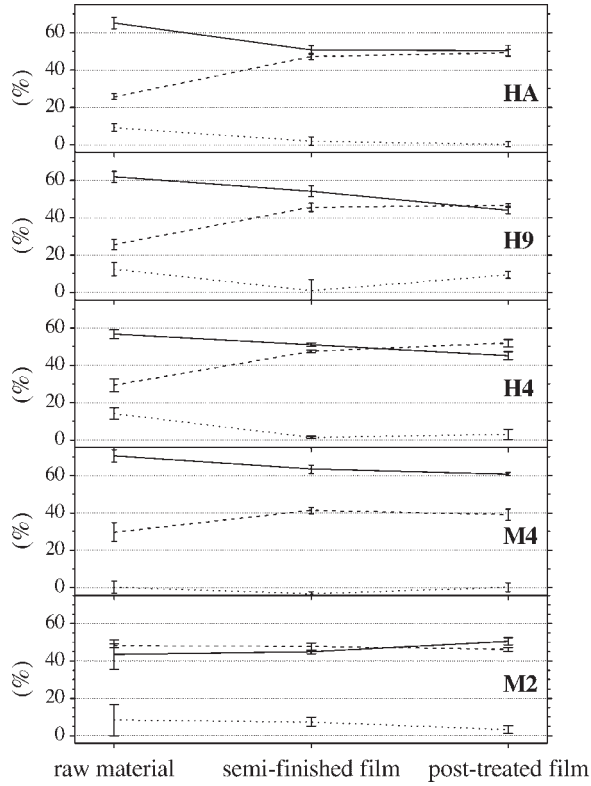

Figure 4.
Crystalline —, amorphous --- and interfacial ····· fractions as a function of processing level.

At semi-finished film level it is remarkable that the various UHMWPE grades investigated exhibit comparable phase fractions. Thus, it can be concluded that the morphology after sintering is not affected by the average molar mass values but by the sinter process. In contrast, after post-treatment different phase fractions were identified for the UHMWPE samples, which can be related to the differences in the molecular structure.

Differential Scanning Calorimetry

In Figure 5 the DSC traces of the investigated PE grades are shown for the various process levels. While the extrusion grade M2 exhibits the lowest melting peak temperatures of about 120 °C, the values of the second extrusion grade M4 are comparable to the melting peak temperatures of the investigated UHMWPE polymers. For all grades extrusion or sintering is associated by a significant shift of the melting

Table 2.
Mean and standard deviation values (%) of the three phase fractions of the investigated materials.

Sample	Raw material			Semi-finished film			Post-treated film		
	α_a	α_b	α_c	α_a	α_b	α_c	α_a	α_b	α_c
M2	48 ± 1	8 ± 8	43 ± 8	48 ± 2	7 ± 2	45 ± 1	46 ± 1	3 ± 2	50 ± 2
M4	30 ± 5	0 ± 3	71 ± 3	41 ± 2	-3 ± 1	63 ± 2	39 ± 3	0 ± 2	61 ± 1
H4	29 ± 3	14 ± 3	57 ± 2	48 ± 1	2 ± 1	51 ± 1	52 ± 2	3 ± 3	45 ± 2
H9	26 ± 3	13 ± 3	62 ± 3	45 ± 2	1 ± 6	54 ± 3	46 ± 1	9 ± 2	44 ± 2
HA	26 ± 2	9 ± 2	65 ± 3	47 ± 2	2 ± 2	51 ± 2	49 ± 2	0 ± 1	50 ± 3

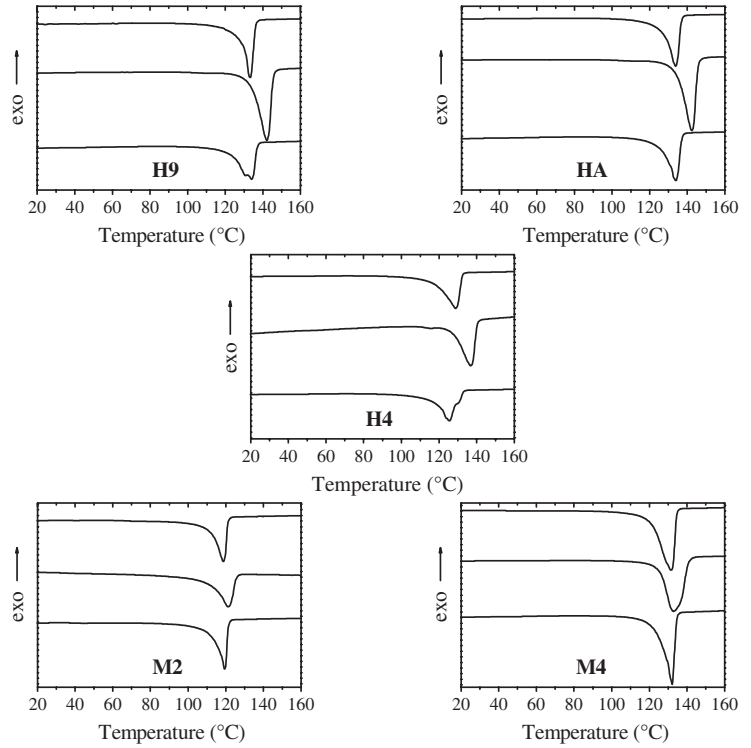

Figure 5.
DSC melting endotherms of the investigated PE grades (M2, M4, H4, H9 and HA) at raw material, semi-finished film and post-treated film level (from bottom to top).

peak to higher temperatures. This shift is most likely attributed to thicker crystal lamellae. However, because of the lower crystalline and interfacial fractions derived from Raman spectroscopy presumably less crystal lamellae are formed associated with thicker amorphous layers, which can be attributed to the different thermal and process histories during polymerization and film production.

For the post-treated films, compared to the semi-finished films, a shift of the melting peak temperatures to lower values is ascertained. Due to flaming the samples were exposed to temperatures above the melting temperature, thus leading to a melting and recrystallization of the film surface. This negative shift is most likely in conjunction with the formation of thinner crystal lamellae. Because of the lower crystalline fractions derived from Raman spectroscopy for many of the investigated PE grades (M4, H4, H9 and HA), a comparable amount of crystal lamellae, but with lower thickness is evolved. The different morphology is probably related to a higher cooling rate during post-treatment.

A comparison of the crystallinity values determined by DSC and Raman spectroscopy is revealed in Figure 6 and summarized in Table 3. In general, a good agreement between the DSC and Raman crystallinities was found, thus corroborating the results obtained by Raman spectroscopy and the assumption of an orthorhombic crystalline structure. With exception of the M2 grade the correlation coefficients are equal to 0.90 or higher. The lower correlation coefficient for the M2 grade is related to the fact that the crystallinity values are within a small range. The tendency for lower Raman crystallinity

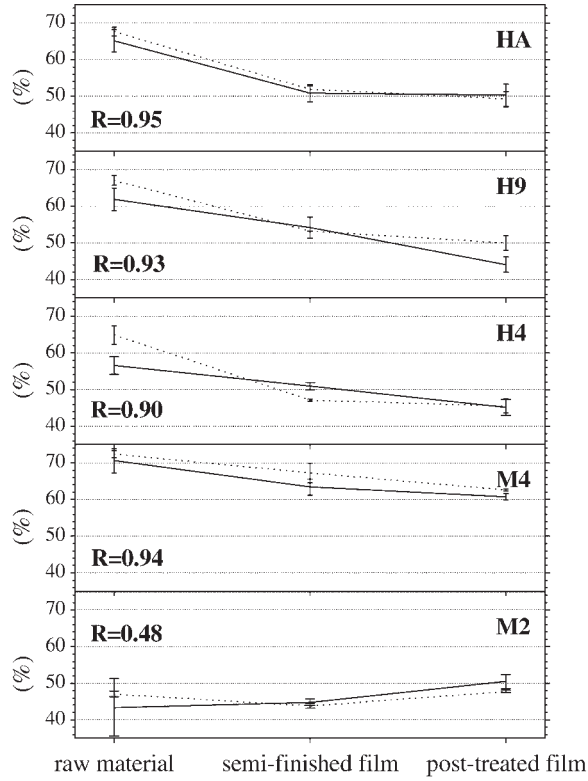

Figure 6.
Crystallinity as a function of processing level of the investigated materials determined by Raman spectroscopy — and DSC ·····; R represents the correlation coefficient between Raman and DSC results.

Table 3.
Mean and standard deviation of the crystallinity values (%) of the investigated materials obtained by DSC and Raman spectroscopy.

Sample	Raw material		Semi-finished film		Post-treated film	
	DSC	Raman	DSC	Raman	DSC	Raman
M2	47 ± 1	43 ± 8	44 ± 1	45 ± 1	48 ± 0	50 ± 2
M4	72 ± 1	71 ± 3	67 ± 3	63 ± 2	63 ± 0	61 ± 1
H4	65 ± 3	57 ± 2	47 ± 0	51 ± 1	46 ± 2	45 ± 2
H9	67 ± 1	62 ± 3	53 ± 0	54 ± 3	50 ± 2	44 ± 2
HA	68 ± 1	65 ± 3	52 ± 1	51 ± 2	49 ± 2	50 ± 3

values compared to DSC reported in the literature[5,11,19] is confirmed to some extent. As discussed in section Raman spectroscopy the crystallinity values are decreasing significantly for the samples M4, H4, H9 and HA along the process chain. In contrast the crystallinity of the M2 grade is nearly unaffected by the various process steps investigated.

Conclusions

For various PE ski base materials it has been demonstrated that Raman spectroscopy allows for a comprehensive morphological analysis obtaining fractions for the crystalline, amorphous and interfacial phase. Crystallinity values derived by Raman spectroscopy are in good agreement with

DSC based data, thus corroborating the implemented and used Raman technique. Along the process chain from the raw material to the post-treated extruded or sintered film for many of the investigated PE grades a decrease of the crystalline and interfacial fraction associated by an increase of the amorphous content was detected. UHMWPE grades with different average molar mass values exhibited morphological differences at raw material and post-treated film level. However, after sintering the phase fractions are comparable and thus independent of the average molar mass.

Acknowledgements: The research work of this paper was performed at the Polymer Competence Center Leoben GmbH (PCCL, Austria) within the framework of the Kplus-program of the Austrian Ministry of Traffic, Innovation and Technology with contributions by the Institute of Materials and Testing of Plastics at the University of Leoben (Austria) and the Fischer GmbH (Austria). The PCCL is funded by the Austrian Government and the State Governments of Styria and Upper Austria. The authors wish to express their acknowledgement to Ao.Univ.-Prof. Dr. Ronald J. Bakker of the Institute of Mineralogy and Petrology at the University of Leoben (Austria) for his cooperation in course of this study.

[1] Association of Plastic Manufacturers in Europe [APME], *"The Compelling Facts About Plastics"*, 2007.
[2] A. Bertoluzza, C. Fagnano, M. Rossi, A. Tinti, G. L. Cacciari, *Journal of Molecular Structure* **2000**, *521*, 89.
[3] S. Affatato, G. Bersaglia, D. Emiliani, I. Foltran, P. Taddei, M. Reggiani, P. Ferrieri, A. Toni, *Biomaterials* **2003**, *24*, 4045.
[4] M. Visentin, S. Stea, M. de Clerico, M. Reggiani, C. Fagnano, S. Squarzoni, A. Toni, *J. Biomater. Appl.* **2006**, *21*(2), 131.
[5] M. Reggiani, A. Tinti, P. Taddei, M. Visentin, S. Stea, M. de Clerico, C. Fagnano, *Journal of Molecular Structure* **2006**, *785*, 98.
[6] M. Kyomoto, Y. Miwa, G. Pezzotti, *J. Biomater. Sci. Polymer Edn.* **2007**, *18*, 165.
[7] G. R. Strobl, W. Hagedorn, *J. Polymer Sci.* **1978**, *16*, 1181.
[8] D. Dothée, M. Berjot, W. Marx, *J. Polymer Degradation and Stability* **1988**, *20*, 149.
[9] F. Rull, A. C. Prieto, J. M. Casado, F. Sobron, H. G. M. Edwards, *J. Raman. Spectrosc.* **1993**, *24*, 545.
[10] C. C. Naylor, R. J. Meier, B. J. Kip, K. P. J. Williams, S. M. Mason, N. Conroy, D. L. Gerrrard, *Macromolecules* **1995**, *28*, 2969.
[11] W. Lin, M. Cossar, V. Dang, J. Teh, *Polymer Testing* **2007**, *26*, 814.
[12] L. Mandelkern, R. G. Alamo, M. A. Kennedy, *Macromolecules* **1990**, *23*, 4721.
[13] M. A. Rodríguez-Pérez, R. A. Campo-Arnáiz, R. F. Aroca, J. A. de Saja, *Polymer* **2005**, *46*, 12093.
[14] M. Pyda, *ATHAS DataBank* **2007**, http://athas.prz.rzeszow.pl.
[15] G. Keresztury, E. Földes, *Polymer Testing* **1990**, *9*, 329.
[16] J. C. Rodriguez-Cabello, J. Martin-Monge, J. M. Lagaron, J. M. Pastor, Macromol, *Chem. Phys.* **1998**, *199*, 2767.
[17] C. Fagnano, M. Rossi, R. S. Porter, S. Ottani, *Polymer* **2001**, *42*, 5871.
[18] J. M. Lagaron, *J. Materials Sci.* **2002**, *37*, 4101.
[19] R. P. Paradkar, S. S. Sakhalkar, X. He, M. S. Ellison, *J. Appl. Polymer Sci.* **2003**, *88*, 545.
[20] M. Zheng, W. Du, *Vibrational Spectroscopy* **2006**, *40*, 219.
[21] T. Yemni, R. L. McCullogh, *J. Polymer Sci.* **1973**, *11*, 1385.
[22] K. M. Furuheim, D. E. Axelson, H. W. Anthonsen, T. Helle, *J. Appl. Polymer Sci.* **2004**, *91*, 218.
[23] L. Kurelec, S. Rastogi, R. J. Meier, P. J. Lemstra, *Macromolecules* **2000**, *33*, 5593.
[24] J. M. Lagaron, N. M. Dixon, W. Reed, J. M. Pastor, B. J. Kip, *Polymer* **1999**, *40*, 2569.
[25] R. J. Meier, *Polymer* **2002**, *43*, 517.

